

Anisotropy of constrained magnetostrictive materials

Chaitanya Mudivartha^{a,*}, Supratik Datta^b, Jayasimha Atulasimha^c, Phillip G. Evans^d,
Marcelo J. Dapino^{d,**}, Alison B. Flatau^{a,b,**}

^a Materials Science and Engineering, University of Maryland, College Park, MD-20742, USA

^b Aerospace Engineering, University of Maryland, College Park, MD-20742, USA

^c Mechanical Engineering, Virginia Commonwealth University, Richmond, VA-23284, USA

^d Mechanical Engineering, The Ohio State University, Columbus, OH-43210, USA

ARTICLE INFO

Article history:

Received 18 November 2009

Received in revised form

14 April 2010

Available online 15 May 2010

Keywords:

Magnetostriction

Magnetoelastic

Magnetocrystalline

Anisotropy

Energy

Delta K

Three-dimensional

ABSTRACT

The magnetic anisotropy of a ferromagnetic material that is free to deform is defined as the effective anisotropy, which is the sum of intrinsic anisotropy and magnetostriction-induced anisotropy. Prior works [1,2] (Baltzer, 1957; Kittel, 1949) indicate that if the material is undeformed then the measured anisotropy is same as its intrinsic anisotropy. When magnetostrictive materials are used as actuators or sensors they are often mechanically loaded, resulting in a restriction on the deformation. To capture their behavior in such scenarios, a modelling approach is required. Therefore, in this work, the thermodynamic accuracy of the common expressions for magnetostriction-induced and stress-induced anisotropies is first investigated. A 3D magnetoelastic model is then developed using Armstrong's implementation of an energy model. This 3D magnetoelastic model is capable of predicting the stresses induced when the magnetostriction of these materials is constrained. Using this model, it is shown that when the bulk magnetostriction of the material is clamped, the measured anisotropy will not in general be the same as the intrinsic anisotropy. It is also shown that when the magnetostriction is clamped at the microscopic level, i.e. if the material is locally constrained at the exchange length scales, then the measured anisotropy is the intrinsic anisotropy.

© 2010 Elsevier B.V. All rights reserved.

1. Introduction

The total energy of a magnetostrictive material is expressed as the sum of effective magnetocrystalline anisotropy E_K^{eff} , exchange E_{exch} , magnetostatic E_{ms} , stress-induced anisotropy E_σ , and magnetic work (Zeeman energy) $W_{mag} = \mu_0 \mathbf{M} \cdot \mathbf{H}$ energies, where $\mathbf{M} = M_s[\alpha_1 \alpha_2 \alpha_3]^T$ is the magnetization, α are the magnetization direction cosines, and \mathbf{H} is the applied magnetic field:

$$E = E_K^{eff} + E_{exch} + E_{ms} + E_\sigma - W_{mag}. \quad (1)$$

While micromagnetic models [3] minimize the energy expression in Eq. (1), most macroscopic models [4–6] neglect the E_{exch} . This is reasonable as the E_{exch} manifests only when there is a magnetization gradient, i.e. near the domain walls, and thus makes up only a small fraction of the total energy of a sample. Further, macroscopic models mentioned above consider only the internal magnetic fields ignoring the demagnetizing effects from the E_{ms} . The energies E_K^{eff} , E_σ and W_{mag} are used in all the models. The E_σ is

sometimes referred to as magnetoelastic energy [7–10]. However, the works of Kittel [2] and Chikazumi [11] show that this is actually the stress-induced anisotropy energy. The expression for the magnetoelastic energy involves strains while the expression for stress-induced anisotropy does not. This apparent contradiction will be explained in Section 2.

The effective magnetocrystalline anisotropy energy E_K^{eff} is defined [1,2] as the anisotropy of a single crystalline magnetos-trictive sample that is allowed to freely deform. For cubic materials, this is expressed as

$$E_K^{eff} = K_1^{eff}(\alpha_1^2\alpha_2^2 + \alpha_2^2\alpha_3^2 + \alpha_3^2\alpha_1^2) + K_2(\alpha_1^2\alpha_2^2\alpha_3^2). \quad (2)$$

The E_K^{eff} is the sum of the anisotropy of an undeformed sample called intrinsic magnetocrystalline anisotropy energy

$$E_K^0 = K_1^0(\alpha_1^2\alpha_2^2 + \alpha_2^2\alpha_3^2 + \alpha_3^2\alpha_1^2) + K_2(\alpha_1^2\alpha_2^2\alpha_3^2), \quad (3)$$

and magnetostriction-induced anisotropy energy

$$\Delta E_K = \Delta K_1(\alpha_1^2\alpha_2^2 + \alpha_2^2\alpha_3^2 + \alpha_3^2\alpha_1^2). \quad (4)$$

The constants K_1 and K_2 are the fourth and sixth order cubic anisotropy constants, respectively. From the above equations,

$$K_1^{eff} = K_1^0 + \Delta K_1. \quad (5)$$

* Corresponding author.

** Principal corresponding authors.

E-mail addresses: chaitanya.mudivartha@gmail.com (C. Mudivartha), dapino.1@osu.edu (M.J. Dapino), aflatau@umd.edu (A.B. Flatau).

Measurements of the anisotropy of samples that are free to deform give the effective anisotropy. The intrinsic anisotropy is then obtained by subtracting the magnetostriction-induced anisotropy, calculated using theoretically derived expression for ΔK_1 [1,2]. The expression for ΔK_1 was derived by Kittel [2] and Chikazumi [11] by calculating the elastic energy due to lattice distortion caused by magnetostriction. However, their derivation did not consider the mechanical work energy due to applied stresses. Also, external stresses were not included in the derivation of the equilibrium strains. Moreover, the expression used for E_σ was derived using only the mechanical strains produced due to applied stresses while ignoring the magnetoelastic strains. Section 2 of this work derives expressions for the E_σ and ΔK_1 while including the mechanical work energy. The resulting expressions are the same as those in the literature and hence their thermodynamic accuracy is verified.

Kittel also indicates that if a sample can be held at constant strain it is possible to experimentally determine the intrinsic anisotropy. Secemski et al. [12] and Kuriki et al. [13] reported that their anisotropy measurements of single crystalline Nickel films were intrinsic anisotropy values instead of effective anisotropy values. They reasoned that because the films used for measurements were fully constrained by the underlying substrates, the films could be assumed as *undeformed* during the measurements. They then added the theoretically calculated magnetostriction-induced anisotropy to their measured values to compare with the bulk values.

Models for prediction of actuation/sensing behavior of magnetostrictive materials often use effective anisotropy energy, which should be valid as long as the modeled samples are not constrained. However, in recent works [14–16] modeled results were shown to agree with the experimental results even for constrained samples leading to an apparent discrepancy. Therefore, in this paper we develop an understanding of how constraining a sample's magnetostriction affects its anisotropy.

In Section 3, the difference between clamping a material at the microscale and macroscale is discussed. The modelling approach to predict the response of the material when clamped microscopically and macroscopically is outlined. Using this model, it is shown that the measured anisotropy will be equal to the intrinsic anisotropy only if the sample is microscopically clamped.

2. Energy derivation

All energy expressions used or derived in this section are for materials with cubic symmetry, as most widely used magnetostrictive materials like Nickel, Terfenol-D and Galfenol are cubic or near-cubic. As discussed in the Introduction, commonly used energy-based models [4–6] use the total energy of the system $E_T(\alpha) = E_K^{\text{eff}} + E_\sigma - \mu_0 \mathbf{M} \cdot \mathbf{H}$. The stress-induced anisotropy energy

$$E_\sigma = -\frac{3}{2}\lambda_{100}\sigma\{\alpha_1^2\gamma_1^2 + \alpha_2^2\gamma_2^2 + \alpha_3^2\gamma_3^2\} - 3\lambda_{111}\sigma(\alpha_1\alpha_2\gamma_1\gamma_2 + \alpha_2\alpha_3\gamma_2\gamma_3 + \alpha_3\alpha_1\gamma_3\gamma_1) \quad (6)$$

was derived in [2,11], where λ_{100} and λ_{111} are the magnetostriction constants and γ are the direction cosines of externally applied stress σ . The internal or dependent state of the system using energy potential E_T is magnetization (α to be more precise). However, nonlinear modelling of the magnetomechanical effect usually involves the calculation of the system's free energy [17], where the internal states are magnetization and strain and the work energy is due to externally applied mechanical stresses and magnetic fields.

Despite using an energy potential that lacks strain as an internal state and not including the mechanical work energy term,

predictions of the models agree well with experiments. The Armstrong model, in particular, has been used quite successfully to model both actuation and sensing behavior of Iron-Gallium alloys [7,14,18,19]. Moreover, the expression for E_σ was derived [2,11] using only the mechanical strain induced by the applied stress while ignoring the magnetoelastic strain. Therefore, the energy expression is re-derived starting with Gibbs free energy with strain and magnetization as the internal states to verify the thermodynamic accuracy of the energy potential E_T .

It is reasonable to assume the process of magnetization (domain reorientation) to be isothermal and that any entropy change associated with it is negligible, thereby reducing the Gibbs free energy to the enthalpy of the system. For a Stoner–Wohlfarth particle [20], the enthalpy \mathcal{H} with natural dependence on field \mathbf{H} and stress σ , using six-element vector notation, is

$$\mathcal{H}(\mathbf{H}, \sigma) = U(\mathbf{M}, \epsilon) - \epsilon \cdot \sigma - \mu_0 \mathbf{M} \cdot \mathbf{H}, \quad (7)$$

where the internal energy U depends on magnetization \mathbf{M} and strain ϵ according to

$$U(\mathbf{M}, \epsilon) = E_K^0(\alpha) + \mathbf{b} \cdot \epsilon + \frac{1}{2}\epsilon \cdot \mathbf{C}\epsilon. \quad (8)$$

The intrinsic anisotropy energy E_K^0 given in Eq. (3) depends on magnetization orientation α alone. The second internal energy term is the magnetoelastic energy $\mathbf{b} \cdot \epsilon$ [21,11], where

$$\mathbf{b} = [B_1(\alpha_1^2 - \frac{1}{3}) \ B_1(\alpha_2^2 - \frac{1}{3}) \ B_1(\alpha_3^2 - \frac{1}{3}) \ B_2\alpha_1\alpha_2 \ B_2\alpha_2\alpha_3 \ B_2\alpha_3\alpha_1]^T. \quad (9)$$

This energy depends on both strain and magnetization orientation through the magneto-mechanical coupling coefficients B_1 and B_2 . The last internal energy term is the elastic energy with the stiffness

$$\mathbf{C} = \begin{bmatrix} c_{11} & c_{12} & c_{12} & 0 & 0 & 0 \\ c_{12} & c_{11} & c_{12} & 0 & 0 & 0 \\ c_{12} & c_{12} & c_{11} & 0 & 0 & 0 \\ 0 & 0 & 0 & c_{44} & 0 & 0 \\ 0 & 0 & 0 & 0 & c_{44} & 0 \\ 0 & 0 & 0 & 0 & 0 & c_{44} \end{bmatrix}. \quad (10)$$

The total magnetic and magneto-mechanical coupling energy E_T , useful for calculating magnetization, will be derived by substituting the stress and field dependent strain into the enthalpy (7) and dropping terms that do not depend on α . From either $\partial U / \partial \sigma = \epsilon$ or $\partial \mathcal{H} / \partial \epsilon = 0$, the equilibrium strain is

$$\epsilon = \mathbf{C}^{-1}\sigma - \mathbf{C}^{-1}\mathbf{b}, \quad (11)$$

$$= \epsilon_{\text{mech}} + \lambda, \quad (12)$$

where the magnetostriction is given by

$$\lambda = \left[\frac{B_1}{c_{12}-c_{11}} \left(\alpha_1^2 - \frac{1}{3} \right) \ \frac{B_1}{c_{12}-c_{11}} \left(\alpha_2^2 - \frac{1}{3} \right) \ \frac{B_1}{c_{12}-c_{11}} \left(\alpha_3^2 - \frac{1}{3} \right) \right. \\ \left. - \frac{B_2}{c_{44}} \alpha_1 \alpha_2 \ - \frac{B_2}{c_{44}} \alpha_2 \alpha_3 \ - \frac{B_2}{c_{44}} \alpha_3 \alpha_1 \right]^T, \quad (13)$$

$$= \left[\frac{3}{2} \lambda_{100} \left(\alpha_1^2 - \frac{1}{3} \right) \ \frac{3}{2} \lambda_{100} \left(\alpha_2^2 - \frac{1}{3} \right) \ \frac{3}{2} \lambda_{100} \left(\alpha_3^2 - \frac{1}{3} \right) \right. \\ \left. 3\lambda_{111}\alpha_1\alpha_2 \ 3\lambda_{111}\alpha_2\alpha_3 \ 3\lambda_{111}\alpha_3\alpha_1 \right]^T. \quad (14)$$

The equilibrium strain derived earlier [2,10,11,22] for zero stress included only the second part of Eq. (11), which is the magnetostrictive strain λ . By including the external stress, it is shown here that the equilibrium strain is a superposition of the purely mechanical ϵ_{mech} and magnetostrictive strains.

Substitution of (11) into (7) and noting that the compliance \mathbf{C}^{-1} is symmetric yields

$$\mathcal{H} = E_K^0 - \frac{1}{2} \mathbf{b} \cdot \mathbf{C}^{-1} \mathbf{b} - \mathbf{C}^{-1} \mathbf{b} \cdot \sigma - \frac{1}{2} \sigma \cdot \mathbf{C}^{-1} \sigma - \mu_0 \mathbf{M} \cdot \mathbf{H}, \quad (15)$$

and using (12)

$$\mathcal{H} = E_K^0 - \frac{1}{2} \lambda \cdot \mathbf{C} \lambda - \lambda \cdot \boldsymbol{\sigma} - \frac{1}{2} \boldsymbol{\sigma} \cdot \mathbf{C}^{-1} \boldsymbol{\sigma} - \mu_0 \mathbf{M} \cdot \mathbf{H}. \quad (16)$$

The strain energy density from magnetostriction depends only on the magnetization orientation and using (13) can be incorporated into the anisotropy energy

$$-\frac{1}{2} \lambda \cdot \mathbf{C} \lambda = \frac{9}{4} [\lambda_{100}^2 (c_{11} - c_{12}) - 2 \lambda_{111}^2 c_{44}] (\alpha_1^2 \alpha_2^2 + \alpha_2^2 \alpha_3^2 + \alpha_3^2 \alpha_1^2) \\ = \Delta K_1 (\alpha_1^2 \alpha_2^2 + \alpha_2^2 \alpha_3^2 + \alpha_3^2 \alpha_1^2). \quad (17)$$

Using $E_K^{\text{eff}} = E_K^0 + \Delta K_1 (\alpha_1^2 \alpha_2^2 + \alpha_2^2 \alpha_3^2 + \alpha_3^2 \alpha_1^2)$, the resulting expression for the enthalpy is

$$\mathcal{H}(\mathbf{H}, \boldsymbol{\sigma}) = E_K^{\text{eff}}(\boldsymbol{\alpha}) - \lambda \cdot \boldsymbol{\sigma} - \frac{1}{2} \boldsymbol{\sigma} \cdot \mathbf{C}^{-1} \boldsymbol{\sigma} - \mu_0 \mathbf{M} \cdot \mathbf{H}, \quad (18)$$

which is thermodynamically accurate since the relations $\partial \mathcal{H} / \partial \boldsymbol{\varepsilon} = 0$ and $\partial \mathcal{H} / \partial \boldsymbol{\sigma} = -\boldsymbol{\varepsilon}$ still hold. Noting that $\mathbf{M} = M_s \boldsymbol{\alpha}$, the equilibrium magnetization orientation can be calculated from $\partial \mathcal{H} / \partial \boldsymbol{\alpha} = 0$. Since the strain is already known, purely mechanical terms are no longer needed. The total magnetic and magneto-mechanical energy is then

$$E_T(\mathbf{H}, \boldsymbol{\sigma}) = E_K^{\text{eff}}(\boldsymbol{\alpha}) - \lambda \cdot \boldsymbol{\sigma} - \mu_0 \mathbf{M} \cdot \mathbf{H}, \quad (19)$$

and the magnetization orientation can be calculated from $\partial E_T / \partial \boldsymbol{\alpha} = 0$. For an applied longitudinal stress σ with direction cosines γ_1 , γ_2 , and γ_3

$$-\lambda \cdot \boldsymbol{\sigma} = E_\sigma = -\frac{3}{2} \lambda_{100} \sigma (\alpha_1^2 \gamma_1^2 + \alpha_2^2 \gamma_2^2 + \alpha_3^2 \gamma_3^2) \\ - 3 \lambda_{111} \sigma (\alpha_1 \alpha_2 \gamma_1 \gamma_2 + \alpha_2 \alpha_3 \gamma_2 \gamma_3 + \alpha_3 \alpha_1 \gamma_3 \gamma_1). \quad (20)$$

For a field H applied with direction cosines β_1 , β_2 , and β_3 the energy is

$$E_T(\mathbf{H}, \boldsymbol{\sigma}) = (K_1 + \Delta K_1) (\alpha_1^2 \alpha_2^2 + \alpha_2^2 \alpha_3^2 + \alpha_3^2 \alpha_1^2) + K_2 (\alpha_1^2 \alpha_2^2 \alpha_3^2) \\ - \frac{3}{2} \lambda_{100} \sigma (\alpha_1^2 \gamma_1^2 + \alpha_2^2 \gamma_2^2 + \alpha_3^2 \gamma_3^2) - 3 \lambda_{111} \sigma (\alpha_1 \alpha_2 \gamma_1 \gamma_2 + \alpha_2 \alpha_3 \gamma_2 \gamma_3 \\ + \alpha_3 \alpha_1 \gamma_3 \gamma_1) - \mu_0 M_s H (\alpha_1 \beta_1 + \alpha_2 \beta_2 + \alpha_3 \beta_3). \quad (21)$$

The 1/3 terms in the magnetostriction (13) have been dropped since they result in purely mechanical terms. The energy (21) with 1D inputs is the expression used in the Armstrong's implementation of the energy model [5]. Any stress state can be decomposed into three principal, longitudinal stresses σ_j with direction cosines $\gamma_{j,1}$, $\gamma_{j,2}$, and $\gamma_{j,3}$. Hence for 3D applications the energy

$$E_T(\mathbf{H}, \boldsymbol{\sigma}) = (K_1 + \Delta K_1) (\alpha_1^2 \alpha_2^2 + \alpha_2^2 \alpha_3^2 + \alpha_3^2 \alpha_1^2) + K_2 (\alpha_1^2 \alpha_2^2 \alpha_3^2) \\ - \sum_{j=1}^3 \left[\frac{3}{2} \lambda_{100} \sigma_j (\alpha_1^2 \gamma_{j,1}^2 + \alpha_2^2 \gamma_{j,2}^2 + \alpha_3^2 \gamma_{j,3}^2) + 3 \lambda_{111} \sigma_j (\alpha_1 \alpha_2 \gamma_{j,1} \gamma_{j,2} \right. \\ \left. + \alpha_2 \alpha_3 \gamma_{j,2} \gamma_{j,3} + \alpha_3 \alpha_1 \gamma_{j,3} \gamma_{j,1}) \right] - \mu_0 M_s H (\alpha_1 \beta_1 + \alpha_2 \beta_2 + \alpha_3 \beta_3), \quad (22)$$

or the expression (19) can be used to calculate the magnetization orientation.

The above derivation assumed that the material's deformation is unconstrained. Therefore, as long as the material is free to deform the measured anisotropy will be the effective anisotropy. It is also clear from the derivation that the expressions for both ΔK_1 and E_σ are thermodynamically consistent.

Kittel [2] and Baltzer [1] described that if the material is held under iso-strain condition then the measured anisotropy should be equal to the intrinsic anisotropy. Therefore, in the next section, the anisotropy of the material whose deformation is constrained is investigated.

3. Magnetoelastic modelling for iso-strain condition

The simplest case of an iso-strain condition is if the initial strain state is zero. Substituting $\boldsymbol{\varepsilon} = 0$ in Eq. (7) and using Eq. (8) yields

$$\mathcal{H} = E_K^0 - \mu_0 \mathbf{M} \cdot \mathbf{H}. \quad (23)$$

The anisotropy contribution to the enthalpy is only from the intrinsic anisotropy of the material. Therefore, if $\boldsymbol{\varepsilon} = 0$ can be maintained then the measured anisotropy will in fact be the intrinsic anisotropy as Kittel and Baltzer described [1,2].

The usual anisotropy measurement procedure is to measure the internal energy at constant strain in two directions and compare the difference with the theoretical expression for anisotropy energy in the two directions, since $U(\mathbf{M}_1, \boldsymbol{\varepsilon}_0) - U(\mathbf{M}_0, \boldsymbol{\varepsilon}_0) = \Delta U = \int_{\mathbf{M}_0}^{\mathbf{M}_1} \mathbf{H} d\mathbf{M}$. If exchange and demagnetizing energies are negligible, then ΔU is a linear combination of the anisotropy constants, thus K_1 and K_2 can be calculated by measuring ΔU for two different endpoints $(\mathbf{M}_0, \mathbf{M}_1)$.

As noted earlier, the enthalpy expression in Eq. (7) gives the energy associated with a Stoner–Wohlfarth particle with magnetization oriented along a direction $\boldsymbol{\alpha}$. The Stoner–Wohlfarth particle is a single domain hypothetical particle of a ferromagnetic material [20]. Since there is always a possibility of a single domain breaking up into multiple domains, one can assume the Stoner–Wohlfarth particle to be of dimensions less than the exchange length. We refer to holding $\boldsymbol{\varepsilon} = 0$ at these length scales as *microscopic clamping*.

In practice, however, bulk or macroscopic quantities are usually measured. For example, a strain gage measures the average strain over the gage area and an induction pick-up coil measures the average induction over its cross-section. We refer to maintaining a constant measured bulk strain as *macroscopic clamping*. To study the effect of using macroscopic quantities with the microlevel (Stoner–Wohlfarth particle) energy, a model is needed for evaluating the macroscopic magnetization $\langle \mathbf{M} \rangle$ and magnetostriction $\langle \lambda \rangle$. In order to do this, the knowledge of equilibrium domain configuration (spatial distribution of moments) is essential. This can be calculated by minimizing the energy in Eq. (1). Zhang et al. [3] performed such a calculation using micromagnetic simulation. Using the equilibrium domain distribution, the macroscopic magnetization and magnetostriction were calculated. However, solving for equilibrium $\boldsymbol{\alpha}$ as a function of \mathbf{x} involves spatial discretization of the sample volume leading to substantial computational times. Therefore, such simulations are suitable only for samples of smaller volumes. Most commonly used magnetomechanical models like Jiles [23], Armstrong [5], and Evans and Dapino [9] use the energy expression (21) ignoring the only term that is spatially dependent E_{exch} . This is a valid approximation as E_{exch} depends on the gradient of $\boldsymbol{\alpha}$ and hence is zero everywhere in the sample except within the domain walls. Since domain walls constitute small fraction of the sample volume, it can be safely ignored. These models also ignore E_{ms} and hence the effects due to the demagnetization fields are not considered. This can be mitigated by performing measurements in closed magnetic circuits. Because of the omission of the spatial energy terms, it is impossible for these models to explicitly calculate the domain configuration. Therefore, they either use an empirical or probability distribution function to overcome this problem.

For example, Jiles [23] calculated the magnetization and magnetostriction of Terfenol-D by using an empirical fit of a Langevin function to measured curves instead of using equilibrium domain configuration. Armstrong [5], on the other hand, calculated the macroscopic magnetization and magnetostriction

using a probabilistic approach. The fractional volumes of the material with moments oriented in a particular direction were calculated using a probability distribution that assigns a higher probability to a direction with lower energy. Evans and Dapino [9] used a similar probabilistic approach but included losses associated with moment flipping between energy wells.

For the purpose of evaluating the $\langle \mathbf{M} \rangle$ and $\langle \lambda \rangle$, we employ the Armstrong model described in detail in the next section.

3.1. Macroscopic magnetization and magnetostriction

To calculate the macroscopic magnetization $\langle \mathbf{M} \rangle$ and magnetostriction $\langle \lambda \rangle$ it is essential to calculate the equilibrium domain configuration by minimizing the energy in Eq. (1). For reasons discussed above, the E_{exch} , which is a function of spatial coordinates and the E_{ms} are ignored and the resulting energy in Eq. (22) is used. As a result, it is impossible to explicitly calculate the domain configuration. Therefore, a probabilistic approach is used to calculate the volume of the material with moments oriented along a particular direction. Lower energy orientations are more probable. This can be quantitatively defined using an exponential probability density function (*pdf*). The probability of the magnetization to be oriented along a direction (θ, ϕ) will therefore be

$$f(\theta, \phi) = \frac{e^{-E_T(\theta, \phi)/\omega}}{\int e^{-E_T(\theta, \phi)/\omega} d\Omega}, \quad (24)$$

where ω is the scale parameter, θ and ϕ are the azimuthal and elevation angles, respectively, and $d\Omega = \sin\theta d\theta d\phi$. The direction cosines α are related to (θ, ϕ) as $\alpha_1 = \sin\theta \cos\phi$, $\alpha_2 = \sin\theta \sin\phi$, and $\alpha_3 = \cos\theta$. Since E_{exch} and E_{ms} , which dictate the domain configuration are ignored, the enthalpy is scaled using ω , which is an empirical parameter such that meaningful probabilities occur in the desired range of energy.

Using the *pdf*, volume $V_{\theta, \phi}$ of the material with magnetization oriented along (θ, ϕ) can be written as

$$V_{\theta, \phi} = Vf(\theta, \phi), \quad (25)$$

where V is the total volume of the sample. Utilizing Eq. (25), the macroscopic magnetization $\langle \mathbf{M} \rangle$ can be calculated as

$$\langle \mathbf{M} \rangle = \frac{1}{V} \int \mathbf{M} V_{\theta, \phi} d\Omega = \int \mathbf{M} f(\theta, \phi) d\Omega. \quad (26)$$

Similar to the calculation of $\langle \mathbf{M} \rangle$, macroscopic magnetostriction $\langle \lambda \rangle$ can be evaluated as

$$\langle \lambda \rangle = \int \lambda f(\theta, \phi) d\Omega. \quad (27)$$

The scale parameter ω is estimated by comparing the model predicted $\langle \mathbf{M} \rangle$ or $\langle \lambda \rangle$ values with measured values. Since this approach does not explicitly calculate the domain configuration rather uses a *pdf* to determine the volume fractions corresponding to different orientations, an error in the modelling is unavoidable. However, this error was shown to be small [5,7].

Thus calculated macroscopic values of magnetostriction $\langle \lambda \rangle$ can be used to evaluate the stress induced when a sample is macroscopically constrained.

3.2. Blocked stress calculation

When the material is blocked, the macroscopic average magnetostriction calculated using Eq. (27) leads to an induced stress. To calculate this induced stress, the constitutive equation, which is a 3D form of Hooke's law relating strain and stress must be used

$$\boldsymbol{\sigma} = \mathbf{C}(\boldsymbol{\varepsilon} - \langle \lambda \rangle_{(\mathbf{H}, \boldsymbol{\sigma})}). \quad (28)$$

When the material is clamped in all directions the total strain equals the pre-strain $\boldsymbol{\varepsilon} = \boldsymbol{\varepsilon}_0$. The pre-strain $\boldsymbol{\varepsilon}_0$ has two components. The first component is the mechanical strain $\mathbf{C}^{-1}\boldsymbol{\sigma}_0$ while the second is the magnetostriction $\langle \lambda \rangle_{(\mathbf{H}_0, \boldsymbol{\sigma}_0)}$ due to the application of pre-stress $\boldsymbol{\sigma}_0$ and initial field \mathbf{H}_0 . Therefore,

$$\boldsymbol{\varepsilon} = \mathbf{C}^{-1}\boldsymbol{\sigma}_0 + \langle \lambda \rangle_{(\mathbf{H}_0, \boldsymbol{\sigma}_0)}. \quad (29)$$

Substituting this into Eq. (28) and subtracting the pre-stress gives the induced stress

$$\boldsymbol{\sigma}_{ind} = \mathbf{C}(\langle \lambda \rangle_{(\mathbf{H}_0, \boldsymbol{\sigma}_0)} - \langle \lambda \rangle_{(\mathbf{H}, \boldsymbol{\sigma})}). \quad (30)$$

For cases where not all the directions are blocked, a constraint vector $[bl_{11} \ bl_{22} \ bl_{33} \ bl_{12} \ bl_{23} \ bl_{13}]$ describing which of the strains are blocked can be defined. For example, $bl_{11}=1$ indicates that ε_{11} is blocked.

If all the strains are blocked ($bl_{ij}=1$) then the total strain is the pre-strain $\boldsymbol{\varepsilon} = \boldsymbol{\varepsilon}_0$ and if none of the strains are blocked ($bl_{ij}=0$) then the total stress is the pre-stress $\boldsymbol{\sigma} = \boldsymbol{\sigma}_0$. For mixed cases where strain along only selected directions is blocked, we can combine the statements for $bl_{ij}=1$ and 0 cases to get

$$\mathcal{A}\mathbf{C}\boldsymbol{\varepsilon} + (\mathbf{I} - \mathcal{A})\boldsymbol{\sigma} = \mathcal{A}\mathbf{C}\boldsymbol{\varepsilon}_0 + (\mathbf{I} - \mathcal{A})\boldsymbol{\sigma}_0, \quad (31)$$

where

$$\mathcal{A} = \begin{bmatrix} bl_{11} & 0 & 0 & 0 & 0 & 0 \\ 0 & bl_{22} & 0 & 0 & 0 & 0 \\ 0 & 0 & bl_{33} & 0 & 0 & 0 \\ 0 & 0 & 0 & bl_{12} & 0 & 0 \\ 0 & 0 & 0 & 0 & bl_{23} & 0 \\ 0 & 0 & 0 & 0 & 0 & bl_{13} \end{bmatrix}. \quad (32)$$

Eqs. (28) and (31) can be represented in a matrix form

$$\begin{bmatrix} \mathbf{C} & -\mathbf{I} \\ \mathcal{A}\mathbf{C} & (\mathbf{I} - \mathcal{A}) \end{bmatrix} \begin{bmatrix} \boldsymbol{\varepsilon} \\ \boldsymbol{\sigma} \end{bmatrix} = \begin{bmatrix} \mathbf{C}\langle \lambda \rangle_{(\mathbf{H}, \boldsymbol{\sigma})} \\ \mathcal{A}\mathbf{C}\boldsymbol{\varepsilon}_0 + (\mathbf{I} - \mathcal{A})\boldsymbol{\sigma}_0 \end{bmatrix}. \quad (33)$$

The strain ($\boldsymbol{\varepsilon}_{ind}$) and stress ($\boldsymbol{\sigma}_{ind}$) induced can be calculated from the total strain ($\boldsymbol{\varepsilon}$) and stress ($\boldsymbol{\sigma}$) evaluated from Eq. (33) by subtracting the pre-strain ($\boldsymbol{\varepsilon}_0$) and pre-stress ($\boldsymbol{\sigma}_0$), respectively,

$$\boldsymbol{\varepsilon}_{ind} = \boldsymbol{\varepsilon} - \boldsymbol{\varepsilon}_0, \quad \boldsymbol{\sigma}_{ind} = \boldsymbol{\sigma} - \boldsymbol{\sigma}_0. \quad (34)$$

The final equation (35) for calculating $\boldsymbol{\varepsilon}_{ind}$ and $\boldsymbol{\sigma}_{ind}$ can be obtained by combining Eqs. (33) and (34)

$$\begin{bmatrix} \boldsymbol{\varepsilon}_{ind} \\ \boldsymbol{\sigma}_{ind} \end{bmatrix} = \begin{bmatrix} \mathbf{C} & -\mathbf{I} \\ \mathcal{A}\mathbf{C} & (\mathbf{I} - \mathcal{A}) \end{bmatrix}^{-1} \begin{bmatrix} \mathbf{C}\langle \lambda \rangle_{(\mathbf{H}, \boldsymbol{\sigma})} \\ \mathcal{A}\mathbf{C}\boldsymbol{\varepsilon}_0 + (\mathbf{I} - \mathcal{A})\boldsymbol{\sigma}_0 \end{bmatrix} - \begin{bmatrix} \boldsymbol{\varepsilon}_0 \\ \boldsymbol{\sigma}_0 \end{bmatrix}. \quad (35)$$

Eq. (35) gives the induced stress ($\boldsymbol{\sigma}_{ind}$) in the material due to $\langle \lambda \rangle_{(\mathbf{H}, \boldsymbol{\sigma})}$ when a magnetic field is applied. Since the energy is also a function of stress, the induced stress changes the E_T and hence $\langle \mathbf{M} \rangle_{(\mathbf{H}, \boldsymbol{\sigma})}$ and $\langle \lambda \rangle_{(\mathbf{H}, \boldsymbol{\sigma})}$. Therefore, in the first iteration the stress in the material is assumed to be the pre-stress $\boldsymbol{\sigma} = \boldsymbol{\sigma}_0$ and then the macroscopic quantities $\langle \mathbf{M} \rangle_{(\mathbf{H}, \boldsymbol{\sigma}_0)}$ and $\langle \lambda \rangle_{(\mathbf{H}, \boldsymbol{\sigma}_0)}$ are evaluated. Using these, the stress in the material is updated as $\boldsymbol{\sigma} = \boldsymbol{\sigma}_0 + \boldsymbol{\sigma}_{ind}$. The updated stress is again used to re-evaluate $\langle \mathbf{M} \rangle_{(\mathbf{H}, \boldsymbol{\sigma})}$ and $\langle \lambda \rangle_{(\mathbf{H}, \boldsymbol{\sigma})}$. This process is iterated until the solution converges as shown in the flow chart in Fig. 1.

4. Results and discussion

From the energy expression derived in Section 2, it can be said that the energy potential often used in magneto-mechanical models is thermodynamically consistent as long as the effective anisotropy is used, i.e., K_1^{eff} . Table 1 shows the reported values of K_1^{eff} along with the calculated values of ΔK_1 using Eq. (17) with values of the magnetostriction and elastic constants for different

cubic magnetostrictive materials. Using ΔK_1 , the intrinsic anisotropy constant K_1^0 is then calculated.

The intrinsic anisotropy constant K_1^0 deviates from the K_1^{eff} by about 0.3% and 10% for Fe and Ni, respectively. However, the deviation for $Tb_{0.3}Dy_{0.7}Fe_{1.9}$, $Fe_{81}Ga_{19}$, and $Fe_{80}Ga_{20}$ is 101%, 31% and 196%, respectively. This shows that while it is not that important whether intrinsic or effective anisotropy values are used for modelling Fe and Ni, it becomes extremely important when dealing with alloys like TbDyFe and FeGa.

To study if the anisotropy of a macroscopically clamped sample is the intrinsic anisotropy only, the magnetoelastic model developed in Section 3 is used. The induced stress σ_{ind} and

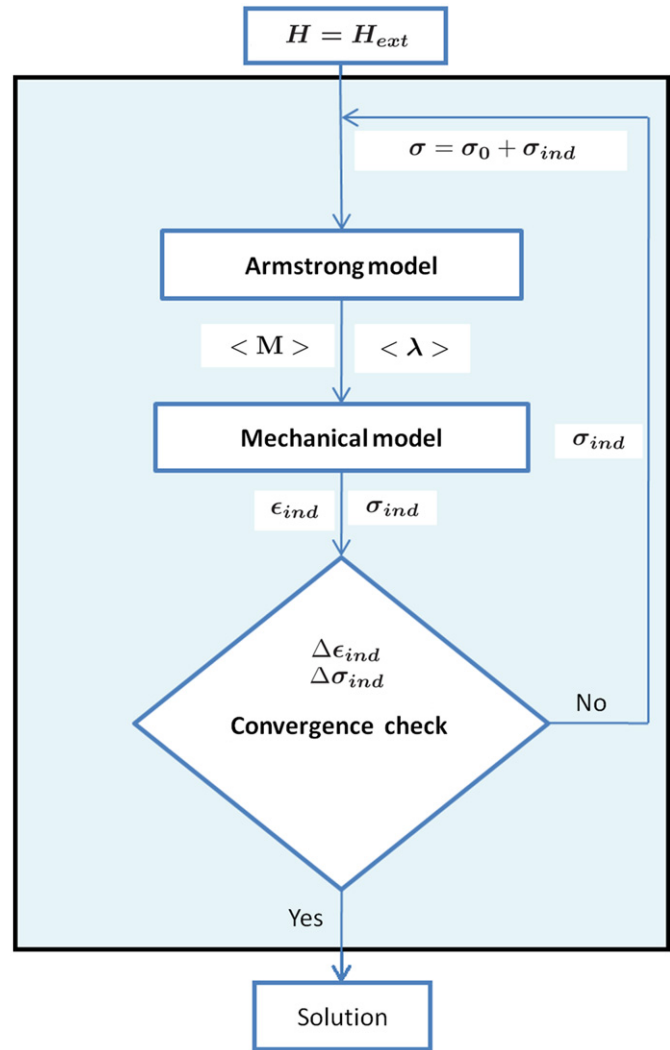


Fig. 1. Flow chart of the model.

Table 1
 ΔK_1 for different materials.

Material	$\frac{1}{2}(c_{11}-c_{12})$	c_{44}	λ_{100}	λ_{111}	K_1^{eff}	ΔK_1	K_1^0
Fe	49 [24]	118 [24]	24 [17]	−23 [17]	48 [17]	−0.154	48.154
Ni	50 [25]	125 [25]	−66 [17]	−29 [17]	5 [17]	0.51	5.51
$Tb_{0.3}Dy_{0.7}Fe_{1.9}$	38 [26]	49 [26]	90 [5]	1840 [5]	−594 [27]	−601	7
$Fe_{81}Ga_{19}$	16 [28]	110 [28]	247 [29]	13 [29]	13 [30]	4.08	8.92
$Fe_{80}Ga_{20}$	12.5 [28]	110 [28]	267 [29]	13 [29]	−2 [30]	3.9	−5.9

Elastic constants c_{11} , c_{12} and c_{44} are in GPa. Magnetostrictive constants λ_{100} and λ_{111} are in ppm. K_1^{eff} , ΔK and K_1^0 are in kJ/m³.

magnetization $\langle \mathbf{M} \rangle$ are calculated as a function of applied magnetic field along the x-direction H_x with the sample constrained in different directions. The x, y, and z axes of the coordinate system are chosen to correspond to the $\langle 100 \rangle$ crystallographic directions of the material. The material is assumed to be $Fe_{81}Ga_{19}$ and the properties listed in Table 1 were used. The pre-stress, pre-strain, and initial magnetic field were all assumed to be zero. The scale parameter ω was chosen as 0.6 kJ/m³ [7]. As described in the model, the process of calculation of induced stress and magnetization is iterated till a converged solution is obtained. The convergence criterion was chosen as $|\Delta \sigma_{ind}| < 0.1\%$ and $|\Delta \epsilon_{ind}| < 0.1\%$. Fig. 2 shows the induced stress for two cases. While case (a) is for the sample clamped only in the x-direction, i.e., for constraint vector [1 0 0 0 0], case (b) is for the sample clamped in all directions, i.e., for constraint vector [1 1 1 1 1].

As expected, when the material is clamped only in the x-direction a compressive stress is induced along this direction. The induced stresses along other directions are zero. When the material is clamped in all directions, compressive stress is induced in the x-direction as its magnetostriction-induced extension along this direction is blocked. As the moments rotate and align along the direction of the field, which is the x-direction, the material contracts along the y and z-directions. With these strains blocked, tensile stresses are induced in these directions. Due to the symmetry of the crystal, the induced stresses in y and z-directions are equal in magnitude.

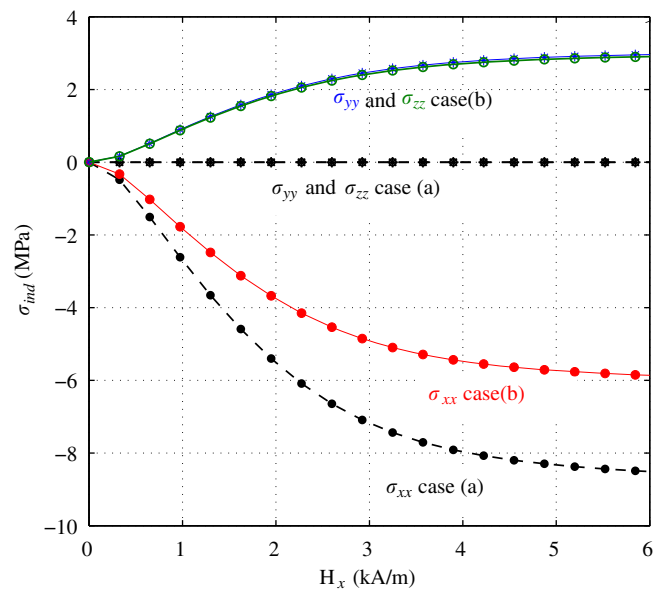


Fig. 2. σ_{ind} – H_x curves for two cases: (a) strain is blocked only in the x-direction; (b) strain is blocked in all directions.

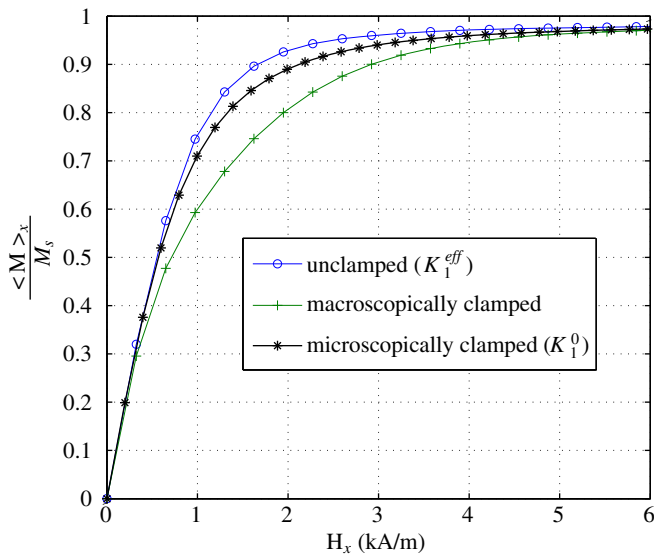


Fig. 3. $\langle M \rangle_x$ – H_x curves for three cases: free or unclamped sample, macroscopically clamped sample, and microscopically clamped sample.

The bulk magnetization along the x -direction $\langle M \rangle_x$ is plotted against the magnetic field applied along the same direction H_x in Fig. 3. The $\langle M \rangle_x$ is plotted for three different cases. The first case is an unconstrained material that is allowed to deform freely, i.e., the constraint vector is $[0 \ 0 \ 0 \ 0 \ 0]$. The second case is a sample clamped macroscopically in all directions, i.e., the constraint vector is $[1 \ 1 \ 1 \ 1 \ 1]$. The third case is a sample clamped microscopically, i.e., the energy shown in Eq. (23) was used. The difference between the M – H curves of microscopically clamped and unconstrained samples can be attributed solely to the ΔK_1 term that is absent in the microscopically clamped case. It can be seen that macroscopic constraining of the sample does not result in the M – H curve matching the microscopically clamped case. This means that the anisotropy measured for the sample that is macroscopically clamped will be different from the intrinsic anisotropy. The reason for this is that when a sample is macroscopically clamped the average strain is maintained constant whereas microscopically the domains are free to rotate. Therefore, although the macroscopic strain is maintained constant the internal strain, locally, is not. The macroscopic clamping case is analogous to the anisotropy introduced by the induced stress that can be calculated using the stress induced anisotropy energy expression with the converged induced-stress values plotted in Fig. 2.

Further, it can be inferred that measuring the magnetic anisotropy of a fully constrained bulk sample will not yield the intrinsic anisotropy. It is plausible the anisotropy is the intrinsic anisotropy if the sample is microscopically clamped. For this, the sample must be locally constrained at the exchange length scales. One possibility of achieving this is by growing a thin film epitaxially on a lattice matching substrate. If the substrate is much thicker than the film, which is usually the case, then the film can be thought to be constrained microscopically. However, the thickness of the film must be restricted to a few monolayers as the lattice can relax the further it is from the film/substrate interface. Since Secemski et al. [12] and Kuriki et al. [13] measured the anisotropy of single crystalline Nickel films constrained by substrates, they did indeed measure the intrinsic anisotropy, which compared well when the ΔK_1 was subtracted from the bulk anisotropy.

The model presented in this work predicts that the anisotropy measurements of $\text{Fe}_{81}\text{Ga}_{19}$ that is macroscopically clamped is

higher than that is unconstrained. To verify this experimentally, bulk $\text{Fe}_{81}\text{Ga}_{19}$ must be encapsulated with a structure of higher stiffness so that the magnetostriction is effectively constrained in all directions. Alternatively, the sample can be constrained along any one direction and an appropriate constraint vector can be used for the model predictions.

5. Conclusions

It is mentioned in literature that the anisotropy of an undeformed magnetostrictive material equals its intrinsic anisotropy as opposed to the effective anisotropy. To model the behavior of constrained samples, it is important to understand whether or not to include ΔK_1 . In prior work, expressions for ΔK_1 and E_σ were both derived without including the mechanical work energy and by considering only the mechanical strains while ignoring the magnetostrictive strains induced by the applied stresses. In this work, an expression for the energy of a ferromagnetic body has been derived starting from the system's Gibbs free energy. It has been shown that the energy potential often used in magneto-mechanical models is thermodynamically accurate as long as the effective magnetostriction-induced anisotropy constant ΔK_1^{eff} is used. It is also shown that the deviation of the intrinsic from the effective anisotropy for Fe–Ga and Tb–Dy–Fe alloys is more than 35% and reaches 200% for Fe–Ga alloys. Therefore, the ΔK_1 is extremely important for giant magnetostrictive materials like Fe–Ga and Tb–Dy–Fe alloys. A model was developed to calculate the bulk magnetization and induced stresses when a sample is clamped. It is shown that when the sample is clamped microscopically, the anisotropy of the material is the intrinsic anisotropy. However, when the sample is clamped macroscopically then the measured anisotropy is neither the intrinsic nor the effective anisotropies. The measured anisotropy is equal to the effective anisotropy plus the stress-induced anisotropy because of the stresses induced as a result of clamping.

Acknowledgements

The authors gratefully acknowledge the support of the US Office of Naval Research through MURI Grant # N000140610530 in funding this research.

References

- [1] P.K. Baltzer, Effective magnetic anisotropy and magnetostriction of mono-crystals, *Physical Review* 108 (3) (1957) 580–587.
- [2] C. Kittel, Physical theory of ferromagnetic domains, *Reviews of Modern Physics* 21 (4) (1949) 541–583.
- [3] J.X. Zhang, L.Q. Chen, Phase-field microelasticity theory and micromagnetic simulations of domain structures in giant magnetostrictive materials, *Acta Materialia* 53 (2005) 2845–2855.
- [4] D. Jiles, J. Thoenke, Theoretical modeling of the effects of anisotropy and stress on the magnetization and magnetostriction of $\text{Tb}_{(0.30)}\text{Dy}_{(0.70)}\text{Fe}_{(1.9-2.0)}$, *Journal of Magnetism and Magnetic Materials* 134 (1994) 143–160.
- [5] W.D. Armstrong, Magnetization and magnetostriction processes in $\text{Tb}_{(0.27-0.30)}\text{Dy}_{(0.73-0.70)}\text{Fe}_{(1.9-2.0)}$, *Journal of Applied Physics* 81 (5) (1997) 2321–2326.
- [6] P.G. Evans, M.J. Dapino, J.B. Restorff, Bill armstrong memorial symposium: free energy model for magnetization and magnetostriction in stressed Gallenol alloys, in: *Proceedings of SPIE, Behavior and Mechanics of Multifunctional and Composite Materials 2007*, vol. 6526, San Diego, California, USA, 2007, pp. 19–29.
- [7] J. Atulasima, A.B. Flatau, J.R. Cullen, Energy-based quasi-static modeling of the actuation and sensing behavior of single-crystal iron-gallium alloys, *Journal of Applied Physics* 103 (1) (2008) 014901 [Online]. Available: <<http://link.aip.org/link/?JAP/103/014901/1>>.
- [8] S. Datta, J. Atulasimha, A.B. Flatau, Modeling of magnetostrictive gallenol sensor and validation using four point bending test, *Journal of Applied Physics* 101 (9) (2007) 09C521–3.

- [9] P.G. Evans, M.J. Dapino, State-space constitutive model for magnetization and magnetostriction of Galfenol alloys, *IEEE Transactions on Magnetics* 44 (7) (2008) 1711–1720.
- [10] E.W. Lee, Magnetostriction and magnetomechanical effects, *Reports on Progress in Physics* 18 (1) (1955) 184–229.
- [11] S. Chikazumi, *Physics of Ferromagnetism*, second ed., Clarendon Press, Oxford, New York, 1997, pp. 350–354, 376–378 (Chapter 14).
- [12] E. Secemski, J.C. Anderson, Magnetic anisotropy in single-crystal nickel films, *Journal of Physics D: Applied Physics* 4 (4) (1971) 574–585 [Online]. Available: <<http://stacks.iop.org/0022-3727/4/574>>.
- [13] S. Kuriki, Strain effects on magnetic anisotropies in (1 1 0) Ni films, *Journal of Applied Physics* 48 (7) (1977) 2992–2997 [Online]. Available: <<http://link.aip.org/link/?JAP/48/2992/1>>.
- [14] C. Mudivarthi, S. Datta, J. Atulasimha, A.B. Flatau, A bidirectionally coupled magnetoelastic model and its validation using a galfenol unimorph sensor, *Smart Materials and Structures* 17 (3) (2008) 035005 (8pp), [Online]. Available: <<http://stacks.iop.org/0964-1726/17/035005>>.
- [15] S. Datta, J. Atulasimha, C. Mudivarthi, A.B. Flatau, The modeling of magnetomechanical sensors in laminated structures, *Smart Materials and Structures* 17 (2) (2008) 025010 (9pp), [Online]. Available: <<http://stacks.iop.org/0964-1726/17/025010>>.
- [16] S. Datta, J. Atulasimha, C. Mudivarthi, A.B. Flatau, Modeling of magnetomechanical actuators in laminated structures, *Journal of Intelligent Material Systems and Structures* 20 (9) (2009) 1121–1135. [Online]. Available: <<http://jim.sagepub.com/cgi/content/abstract/20/9/1121>>.
- [17] G. Engdahl, *Handbook of Giant Magnetostrictive Materials*, first ed., Academic Press, New York, 2000 (Chapter 1).
- [18] J. Atulasimha, A.B. Flatau, E. Summers, Characterization and energy-based model of the magnetomechanical behavior of polycrystalline iron-gallium alloys, *Smart Materials and Structures* 16 (4) (2007) 1265–1276.
- [19] C. Mudivarthi, P. Downey, A.B. Flatau, Elastic and magneto-elastic modeling of galfenol nanowires, in: *Proceedings of SPIE, Nanosensors, Microsensors, and Biosensors and Systems*, vol. 6528, San Diego, CA, USA, 2007, pp. 652 803–11.
- [20] E.C. Stoner, E.P. Wohlfarth, A mechanism of magnetic hysteresis in heterogeneous alloys, *Philosophical Transactions of the Royal Society of London. Series A, Mathematical and Physical Sciences* 240 (826) (1948) 599–642 [Online]. Available: <<http://rsta.royalsocietypublishing.org/content/240/826/599.abstract>>.
- [21] L. Néel, Anisotropie magnétique superficielle et surstructures d'orientation, *Journal de Physique et le Radium* 15 (4) (1954) 225–239.
- [22] E. Kneller, *Ferromagnetismus*, Springer-Verlag, Berlin, 1962, pp. 231–234 (Chapter 16).
- [23] D.C. Jiles, Theory of the magnetomechanical effect, *Journal of Applied Physics* 28 (8) (1995) 1537.
- [24] J.A. Rayne, B.S. Chandrasekhar, Elastic constants of iron from 4.2 to 300 K, *Physical Review* 122 (6) (1961) 1714–1716.
- [25] J.S. Koehler, Attempt to design a strong solid, *Physical Review B* 2 (2) (1970) 547–551.
- [26] A.E. Clark, *Ferromagnetic Materials*, in: E.P. Wohlfarth (Ed.), vol. 1, North-Holland Publishing Company, Amsterdam, 1980, pp. 531–589 (Chapter 7).
- [27] J. Wang, The correlation between the first magnetocrystalline anisotropy constant k_1 and the composition of giant magnetostrictive alloy Tb–Dy–Fe, *Journal of alloys and compounds* 429 (1–2) (2007) 56–59.
- [28] M. Wuttig, L. Dai, J. Cullen, Elasticity and magnetoelasticity of Fe–Ga solid solutions, *Applied Physics Letters* 80 (7) (2002) 1135–1137.
- [29] A.E. Clark, K.B. Hathaway, M. Wun-Fogle, J.B. Restorff, T.A. Lograsso, V.M. Keppens, G. Petculescu, R.A. Taylor, Extraordinary magnetoelasticity and lattice softening in bcc Fe–Ga alloys, *Journal of Applied Physics* 93 (10) (2003) 8621–8623.
- [30] S. Rafique, J.R. Cullen, M. Wuttig, J. Cui, Magnetic anisotropy of FeGa alloys, *Journal of Applied Physics* 95 (11) (2004) 6939–6941.